Solid-State Electronics 56 (2011) 116–119

Contents lists available at ScienceDirect

Solid-State Electronics

journal homepage: www.elsevier.com/locate/sse

Transconductance characteristics and plasma oscillations in nanometric InGaAs field effect transistors

J.-F. Millithaler [a,*], J. Pousset [a], L. Reggiani [a], H. Marinchio [b], L. Varani [b], C. Palermo [b], P. Ziade [c], J. Mateos [d], T. González [d], S. Perez [d]

[a] Dipartimento di Ingegneria dell'Innovazione and CNISM, Università del Salento, Lecce, Italy
[b] Institut d'Electronique du Sud, UMR CNRS 5214, Université Montpellier II, place Bataillon, 34095 Montpellier Cedex 5, France
[c] Laboratoire de Physique Appliquée, Faculté des Sciences II, Université Linbanaise, Fanar, Lebanon
[d] Departamento de Fisicà Aplicada, Universidad de Salamanca, Pza. Merced s/n 37008 Salamanca, Spain

ARTICLE INFO

Article history:
Received 14 May 2010
Received in revised form 1 September 2010
Accepted 1 November 2010
Available online 3 December 2010

The review of this paper was arranged by Prof. S. Cristoloveanu

Keywords:
Plasma
TeraHertz
FET

ABSTRACT

By Monte Carlo simulations we investigate the plasma spectrum in *n*-type InGaAs field effect transistors at 300 K in the whole region of operating conditions from ohmic to saturation regime of the transconductance characteristics. The presence of a two dimensional (2D) plasma peak predicted within the gradual channel approximation is confirmed by the microscopic model and its properties are analyzed systematically. At the highest gate voltages the 2D peak is found to become practically independent of the channel width.

1. Introduction

Generation and detection of electromagnetic radiation in the TeraHertz (THz) domain is a subject in fast development because of its potential applications in different branches of advanced technologies, such as broad-band communications, high-resolution spectroscopy, medical and biological imaging, and security [1–4]. As a consequence, the realization of solid-state devices operating in the THz domain at room-temperature and with compact, powerful, and tunable characteristics is a mandatory issue. To this purpose, one of the most promising strategies lies in the plasmonic approach, which exploits the plasma frequency associated with long range Coulomb interaction of charge carriers as a possible mechanism for THz detection/generation [5,6].

For the case of a field effect transistor (FET), within the gradual channel approximation (GCA) the two dimensional (2D) electron gas in the channel was found to behave as the support of 2D plasma waves with fundamental frequency [7]

$$f_p = \frac{1}{2\pi}\sqrt{\frac{e^2 n_0^{2D} dk^2}{m_0 m \varepsilon_0 \varepsilon_{diel}}} \tag{1}$$

where e is the absolute value of the electron charge, m_0 and m are the free and effective electron masses, respectively, d is the gate to channel distance,

$$n_0^{2D} = \int_0^W n^{3D}(y)dy \tag{2}$$

is the average 2D carrier concentration associated with the thickness W of the channel measured along the y direction, ε_0 is the vacuum permittivity, ε_{diel} is the relative dielectric constant of the dielectric placed in between the gate and the channel and k is the plasma wavevector. Expression (1) was obtained for boundary conditions corresponding to a constant value of the potential at the source and a constant value of the current at the drain contact, respectively. We notice that a practical realization of these boundary conditions within a Monte Carlo (MC) simulator remains an open problem. The 2D plasma frequency is dispersive, i.e. $f_p = f_p(k)$, and, in particular, depends on the geometry of the semiconducting channel and the relative dielectric constant of the external dielectric. Through these plasma oscillations, nanometric High Electron Mobility Transistors (HEMT) provided experimental evidence as emitters and/or detectors of electromagnetic radiation in the THz range [8–10].

In the GCA, since n_0^{2D} can be expressed as UC/e, with $U = U_G - U_C - U_T$, where U_T is the threshold voltage, $(U_G - U_C)$ is the gate to channel voltage, and $C = \varepsilon_0\varepsilon_{diel}/d$ is the gate to channel

* Corresponding author. Tel.: +39 0832 297763; fax: +39 0832 297733.
E-mail address: jf.millithaler@unisalento.it (J.-F. Millithaler).

0038-1101/$ - see front matter © 2010 Elsevier Ltd. All rights reserved.
doi:10.1016/j.sse.2010.11.003

capacitance per unit surface, the 2D plasma frequency can be also conveniently expressed as [7]:

$$f_p = \sqrt{\frac{eU}{m_0 m}} \times \frac{k}{2\pi}. \quad (3)$$

Following the results of a previous research [3], this work investigates the effect of the gate voltage upon the plasma dispersion from a microscopic point of view, thus testing the predictions of the simplified analytical approaches and providing more physical insight into the problem. To this purpose, we consider a FET with a *n*-type $In_{0.53}Ga_{0.47}As$ layer within a gated configuration at room temperature, and investigate the plasma frequency characteristics by analyzing the frequency spectrum of voltage fluctuations extracted from inside the channel (preferably in the center) obtained from a MC simulator coupled with a 2D Poisson solver. As boundary conditions we follow previous works on the subject and use an Ohmic contact at the source (zero constant voltage) and a constant applied voltage at the drain [2]. Contacts are permeable to carriers crossing in both longitudinal directions, while in the transverse direction at the interfaces carriers are reflected inside the channel. Accordingly, the random motion of free carriers is responsible of voltage fluctuations inside the channel, and the redistribution of the electric field associated with the geometry of the sample leads to a modulation of the plasma frequency with respect to its three dimensional (3D) value. The analogous case of an ungated structure was already considered in a previous publication [11] and it can be a valuable source of comparison with present findings.

The paper is organized as follows: the next section reports the results of numerical simulations that are compared with analytical expectations carried out within the GCA. Major achievements are summarized in the conclusions.

2. Results and discussion

Fig. 1 shows a sketch of the structure under simulation. As typical values of the parameters, if not stated otherwise, we take: the gate to channel length d = 20 nm, the channel thickness W = 10 nm, the channel length L = 500 nm, the ionized donor concentration in the channel $N_d = 10^{18}$ cm^{-3} and a drain source voltage of 0.1 V.

Fig. 2 reports the transconductance characteristics of the FET for different values of the source–drain voltage U_D. The behavior of the drain current, I_D, is that typical of a FET. At negative values of U_G one can infer the value of the threshold voltage, $U_T = -3.5$ V, in good agreement with the theoretical expression $U_T = -eN_dWd/(\varepsilon_0\varepsilon_{diel})$. Then, at increasing U_G different curves exhibit an initial linear increase of I_D associated with the increase of free carrier concentration and a subsequent saturation regime that, at the highest values of U_D, is associated with the free carrier concentration at the contacts and the saturation value of the drift velocity.

Fig. 3 reports the plasma spectra pertaining to voltage fluctuations extracted at different points along the channel. We notice that the lowest 2D and the highest 3D peaks remain fixed at the respective values of 3.8 and 11 THz. By contrast, in the intermediate frequency region we observe structures of the spectrum that depend on the position of the voltage extraction. In other words, we can associate the presence of harmonics with different extracting points in qualitative agreement with theoretical predictions of Ref. [12]. The results shown from now on, have been extracted at the central position of each simulated channel.

Fig. 4 compares the spectral densities of voltage fluctuations obtained under different but complementary conditions. The interesting conclusion coming out from the comparison is that the

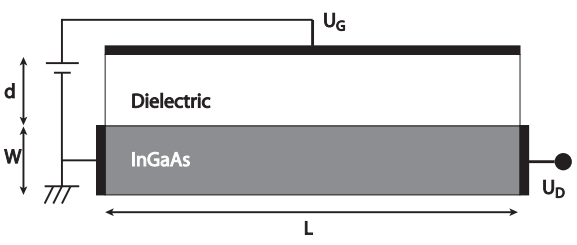

Fig. 1. Scheme of the gated structure with the three terminals.

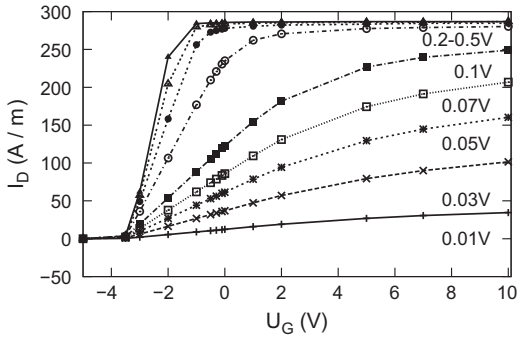

Fig. 2. Transconductance characteristics of the FET for different values of the drain voltage.

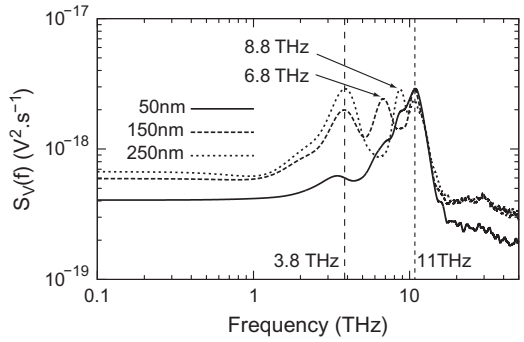

Fig. 3. Plasma structures pertaining to voltage fluctuations extracted at different points (50, 150 and 250 nm) along the channel for L = 500 nm, U_D = 0.01 V, U_G = 0.1 V.

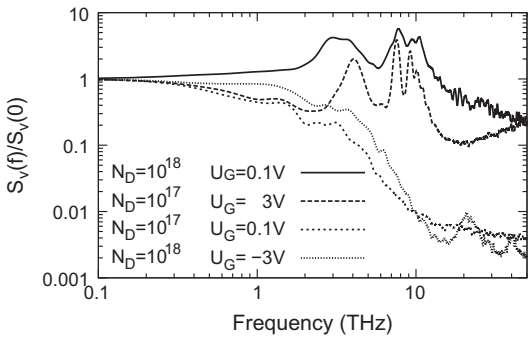

Fig. 4. Spectral density of voltage fluctuations normalized to their static value obtained for different but complementary conditions and U_D = 0.1 V. (a) The continuous curve refers to a negligible gate voltage and a carrier concentration equal to that of the doping of 10^{18} cm^{-3}, which is confirmed by the simulation; (b) the dashed curve refers to a positive gate voltage that enhances the equilibrium carrier concentration of 10^{17} cm^{-3} to an average value of 10^{18} cm^{-3}; (c) the dotted curve refers to a negligible gate voltage and a carrier concentration equal to that of the doping of 10^{17} cm^{-3}, which is confirmed by the simulation; (d) the small-dashed curve refers to a negative gate voltage that depletes the equilibrium carrier concentration of 10^{18} cm^{-3} to an average value of 10^{17} cm^{-3}.

spectra corresponding to a free carrier concentration of 10^{17} cm^{-3} in the channel is practically independent whether the carrier concentration is the same of the donors one, $N_d = 10^{17}$ cm^{-3}, or that associated with a donor concentration of $N_d = 10^{18}$ cm^{-3} and in the presence of a corresponding depletion of free carriers driven by a substantially negative gate voltage. The same conclusion holds by comparing the opposite case corresponding to a free carrier concentration of 10^{18} cm^{-3} in the channel independently whether the carrier concentration is the same of the donors one, $N_d = 10^{18}$ cm^{-3}, or that associated with a donor concentration of $N_d = 10^{17}$ cm^{-3} and in the presence of a corresponding accumulation of free carriers driven by a substantially positive gate voltage.

The good agreement between the two couples of spectra proves the equivalence between a concentration controlled by the gate voltage or by the ionized donors. Furthermore, results show that no plasma peaks over the static plateau of the spectrum are detectable for carrier concentrations below about $n = 10^{17}$ cm^{-3}.

Fig. 5 reports the 2D plasma frequency calculated from Eq. (1) or Eq. (3), taking $k = \pi/(\sqrt{2}L)$ as in Ref. [11] and from the spectra of voltage fluctuations obtained by MC simulations. The agreement between theory and simulations is qualitatively good apart a discrepancy in excess at worst of 15% for the MC values. This discrepancy is mostly associated with the fact that the free carrier concentration along the transverse direction of the channel becomes significantly peaked near to the interface with the dielectric. We conclude that the overall agreement validates the microscopic interpretation of Eqs. (1) and (3) which received some experimental check in references [9,10].

Fig. 6 reports the potential U, calculated as $U \approx U_G - U_T$ since U_C takes negligible values (at most of 0.16 V for $U_G = 10$ V), and from its expression within the GCA $U = en_0^{2D}d/(\epsilon_0\epsilon_r)$ with n_0^{2D} determined from Eq. (2). The good agreement between the values obtained from the two definitions represents a valuable check of consistency and validates from a microscopic point of view the GCA in the region of considered gate voltages.

Fig. 7 reports the average 3D concentration profile versus the transversal channel position for a 10 nm channel thickness as obtained by MC simulations at the reported gate voltages. The different curves illustrate the accumulation/depletion of carriers near to the interface between the channel and the dielectric associated with positive/negative values of the gate voltages.

Fig. 8 reports the average 3D concentration profile along the channel length at the given values of the gate potential. Different curves illustrate the rather uniform concentration along the longitudinal direction, and the accumulation (depletion) effect associated with the positive (negative) values of the gate voltages.

Fig. 9 reports the plasma spectra under an accumulation gate voltage of 10 V for different thicknesses of the channel. The results prove that for $U_G = 10$ V the 2D value of the plasma peak, centered at about 7 THz, is rather independent of the channel thickness. Furthermore, the peaks at the highest frequencies are reminiscent of the 3D value of the plasma frequency.

Fig. 10 reports the plasma peak at the lowest frequency as a function of the channel width for different gate voltages. The results complement those of Fig. 9. Indeed, the simulations evidence that the gated 2D plasma frequency: (i) increases systematically with the thickness (as expected since n_0^{2D} increases with W) at a given gate voltage and, (ii) tends to saturate at the 3D value of about 11 THz that corresponds to an average carrier concentration of 10^{18} cm^{-3}. As shown in Fig. 7, these results are associated with a

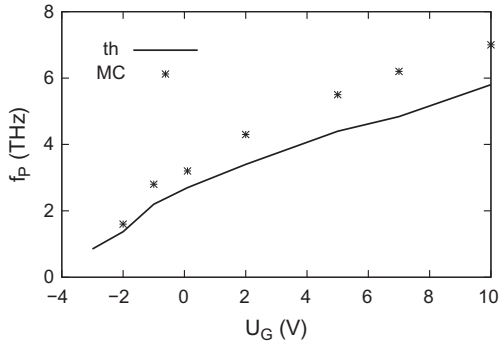

Fig. 5. 2D plasma frequency as a function of the gate voltage. Theoretical values (continuous curve) are calculated using Eq. (2) with the 2D average carrier concentration in the channel obtained by the simulations; numerical values (symbols) correspond to the peak at the lowest frequency evidenced by the spectra of voltage fluctuations provided by MC simulations.

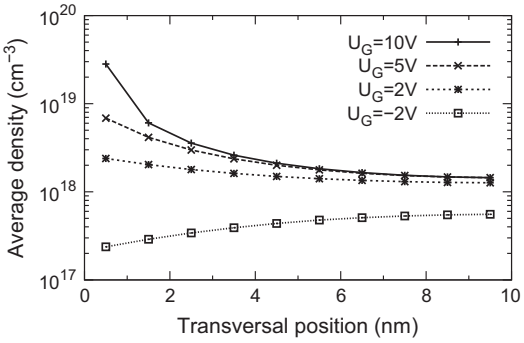

Fig. 7. Profiles of the 3D average concentration of free carriers along the channel thickness when going from the interface with the external dielectric to the other side of the channel. Results are obtained by MC simulations at the reported gate voltages.

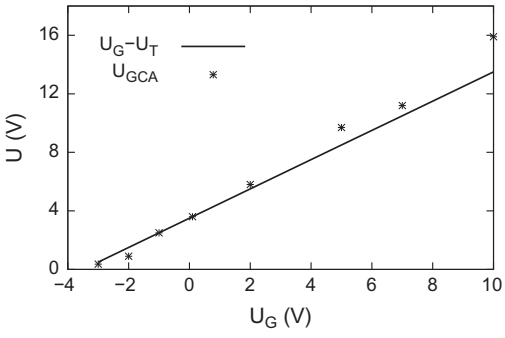

Fig. 6. Potential U as a function of the gate voltage. The continuous line refers to the values obtained from its definition $U = U_G - U_C - U_T$ with $U_C = 0$ and $U_T = -3.5$ V; symbols refer to values obtained within the GCA as $U = en_0^{2D}d/(\epsilon_0\epsilon_r)$ with n_0^{2D} calculated from Eq. (2) using the concentration profiles of MC simulations.

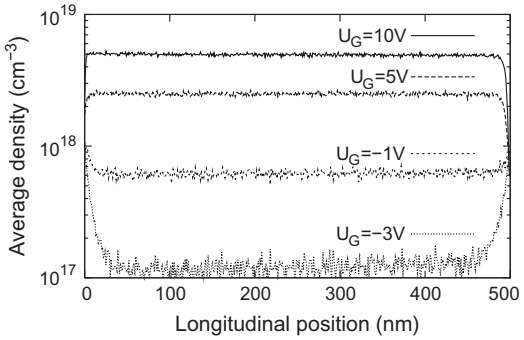

Fig. 8. Profiles of the 3D average concentration of free carriers along the channel length. Results are obtained by MC simulations at the reported gate voltages.

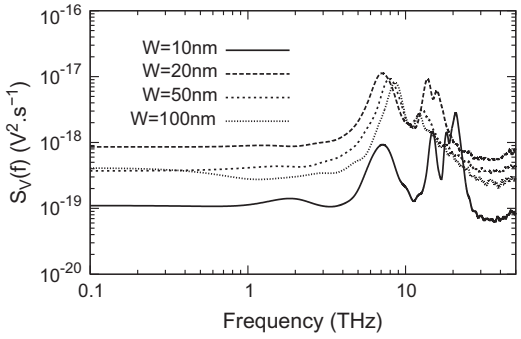

Fig. 9. Spectral density of voltage fluctuations evidencing the plasma peaks under an accumulation gate voltage of 10 V for different thicknesses of the channel.

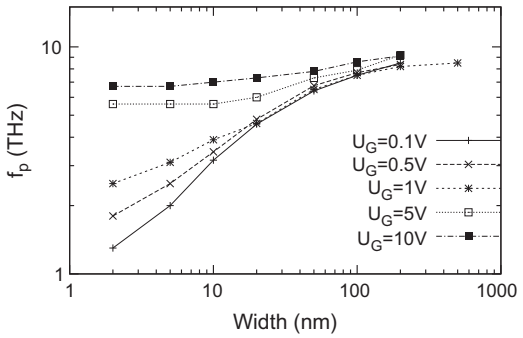

Fig. 10. Plasma peak at the lowest frequency as a function of the channel thickness for different gate voltages and a channel length of 500 nm with $N_d = 10^{18}$ cm^{-3} in the channel.

nonuniform carrier concentration along the channel thickness, and which makes the average 3D carrier concentration at the highest gate voltages rather independent of the thickness in the range $W \leqslant 20$ nm. For values of W larger than about 50 nm, the 2D plasma frequency tends to the 3D value as expected.

3. Conclusion

The paper investigates plasma oscillations in nanometric FETs of InGaAs under a wide range of operating conditions ranging from Ohmic to saturation regime of the transconductance characteristics. The microscopic model makes use of a Monte Carlo simulator self-consistently coupled with a 2D Poisson solver. Simulations are favorably compared with analytical expressions obtained within the gradual channel approximation. Results show that the peak of the plasma frequency can be controlled by means of the gate voltage as long as the channel is near to pinch-off. For high values of $U_G - U_T$, the value of the plasma frequency diverges from the ideal theory [7], and it is found to become nearly independent of the gate voltage and the channel thickness. Here, because of strong charge accumulation just under the interface between the dielectric and the gate, the 2D plasma peak takes values close to that of the 3D peak.

Some hints and guidelines to take advantages of driving 2D plasma frequency by appropriate gate voltages in the range −2 to 10 V and source–drain voltage in the range 10–200 mV are summarized as follows:

- 3D concentration over 10^{16} cm^{-3} is necessary for the plasma peak to be not hidden by thermal noise;
- a reasonable good resolution of 2D plasma frequency over thermal noise is found for channel width in the range 2–20 nm and channel length in the range 100–500 nm.

Acknowledgements

The work was supported by Lavoisier Grant (J. Pousset), CNRS GDR-E Projects "Semiconductor sources and detectors of THz frequencies", Region Languedoc-Roussillon – project "Plateforme Technologique THz", the Dirección General de Investigación (MEC, Spain), FEDER through the project TEC2007-61259/MIC, Accion Integrada HF2007-0014 and by the Consejera de Educación of the Junta de Castilla y León (Spain) through the Projects SA019A08 and GR270.

References

[1] Woollard DL, Brown ER, Pepper M, Kemp M. Terahertz frequency sensing and imaging: a time of reckoning future applications? Proc IEEE 2005;93(10):1722.
[2] Heterostructures terahertz devices, J. Phys: Condens Matter, V. Ryzhii guest editor, 20 (2008) 380301.
[3] Pousset J, Millithaler J-F, Reggiani L, Sabatini G, Palermo C, Varani L, et al. Plasmonic noise in Si and InGaAs semiconductor nanolayers. J Phys: Conf Ser 2009;193:012091.
[4] Klimenko OA, Mityagin Yu A, Videlier H, Teppe F, Dyakonova NV, Consejo C, et al. Terahertz response of InGaAs field effect transistors in quantizing magnetic fields. Appl Phys Lett 2010;97:0022111.
[5] El Fatimy A, Tauk R, Boubanga S, Teppe F, Dyakonova N, Knap W, et al. Plasma oscillations in nanotransistors for room temperature detection and emission of terahertz radiation. Phys Status Solidi (c) 2008;5(1):244–8.
[6] El Fatimy A, Dyakonova N, Meziani Y, Otsuji T, Knap W, Vandenbrouk S, et al. AlGaN/GaN high electron mobility transistors as a voltage-tunable room temperature terahertz sources. J Appl Phys 2010;107:024504.
[7] Dyakonov M, Shur MS. Shallow water analogy for a ballistic field effect transistor: new mechanism of plasma wave generation by dc current. Phys Rev Lett 1993;71:2465.
[8] Lusakowski J, Knap W, Dyakonova N, Varani L, Mateos J, González T, et al. Voltage tuneable terahertz emission from a ballistic nanometer InGaAs/InAlAs transistor. J Appl Phys 2005;97:064307.
[9] Knap W, Deng Y, Rumyantsev S, Shur M. Resonant detection of subterahertz and terahertz radiation by plasma waves in submicron field-effect transistors. Appl Phys Lett 2002;81:24.
[10] Knap W, Lusakowski J, Parenty T, Bollaert S, Cappy A, Popov VV, et al. Terahertz emission by plasma waves in 60 nm gate high electron transistors. Appl Phys Lett 2004;83:13.
[11] Millithaler J-F, Reggiani L, Pousset J, Varani L, Palermo C, Knap W, et al. Monte Carlo investigation of terahertz plasma oscillations in ultrathin layers of n-type $In_{0.53}Ga_{0.47}As$. Appl Phys Lett 2008;92:042113.
[12] Shiktorov P, Starikov E, Gruzhinskis V, Varani L, Sabatini G, Marinchio H, et al. Problems of noise modeling in the presence of total current branching in high electron mobility transistor and field-effect transistor channels. J Stat Mech 2009:P01047.